# Ferroelectric nanoscale logic gates by mixed dislocations in SrTiO₃

Kairi Masuda ⬤,[*] Takahiro Shimada ⬤, and Takayuki Kitamura

*Department of Mechanical Engineering and Science, Kyoto University, Nishikyo-ku, Kyoto 615-8540, Japan*

Conventional nanoscale logic gates involve several critical challenges, such as the appearance of leakage currents, and so new approaches to logic calculation devices have been exploited. However, although polarization switching in ferroelectrics has certain advantages in this regard, including nonvolatility, these materials are not leading candidates for logic gates because they disappear at the nanoscale and do not typically allow the two-inputs–one-output operation which is necessary for logic gates. Here, we demonstrate the possibility that ultrasmall ferroelectric nanoscale logic gates can be generated from mixed dislocations in SrTiO₃. Phase-field simulations show that the unique strain field associated with a mixed dislocation induces a few nanometer polarization spiral, the chirality of which can be switched by electric fields that are both horizontal and vertical to the spiral. Due to this polarization structure, OR, AND, and NOT operations can be performed depending on the strength of the electric fields. These results suggest a different means of fabricating ultrathin logic gates, and could potentially lead to energy-efficient ultrahigh logic density devices.

## I. INTRODUCTION

Logic gates, which perform logical operations such as AND and OR based on a binary system, are the central elements in computational devices. A conventional logic gate comprises several complementary metal-oxide-semiconductor (CMOS) transistors in which the electric currents between the source and drain are controlled by the gate voltage. There has been significant work to date focused on increasing the number of calculations per unit area in these devices by reducing the size of the logic gates, such that these units presently have nanometer-scale dimensions. However, as the size of the gate decreases, leakage currents [1] and heat generation [2] become more problematic. Moreover, so long as logic gates function based on electric currents, they are limited by the Boltzmann tyranny that imposes a fundamental lower limit on the operating voltage [3,4]. These challenges prevent the use of input voltages below approximately 0.5 V and limit the size of standard transistors to greater than 10 nm [5,6]. Consequently, a new approach to logic calculations in nanodevices is required, and spin-current- and magnon-based logic gates and so on have been proposed [7–10]. However, nanoscale logic gates utilizing ferroelectric and similar systems are still in an infancy stage [11–13] even though they have several advantages, including nonvolatile 1 and 0 values represented by polarization [14], relatively low polarization switching energies [15], and no input voltage limitations. This lack of research can be attributed to the fact that, although logic calculations generally use two inputs to obtain a single output, in a typical dipole system one output is determined by one input. As an example, the *c*-axis polarization in ferroelectrics can be switched only by the electric field along the same *c*-axis and not the fields in other directions [16].

Furthermore, the issue of scalability should be mentioned, that is, the ultimate size of logic circuits is one of the central issues in the search for alternative logic gates because it determines computation ability per area. The most excellent scalability was recently demonstrated by a logic gate with a layered structure of multiferroics and topological materials that convert spin to charge [11]. They successfully demonstrated that the components of logic circuits can be miniaturized to the 10-nm scale. However, this study indicates at the same time that, regardless of the mechanisms, the scalability brought by the miniaturization of external shapes or circuits will meet the critical size of a few ten nanometers the same as CMOS because material properties begin to be disturbed or disappear at this scale. This includes ferroelectrics because they disappear below a critical thickness of 5–10 nm [17–19].

It has been reported that nanoscale ferroelectrics can be realized by taking advantage of dislocations, which are atomic-level imperfections and often degrade material properties [20–22]. Strontium titanate (SrTiO₃) exhibits ferroelectric properties when subjected to mechanical strain above a specific level, but remains in the paraelectric state under unstressed conditions [23–25]. As a result of this intriguing multiphysics property, ferroelectricity can be induced on a scale of only several nanometers via strain concentration around a dislocation [26,27]. First-principles calculations for SrTiO₃ have shown that rectilinear polarization vertical to the dislocation line is induced around an edge dislocation, while spiral polarization horizontal to the line is induced around a screw dislocation [28]. Therefore, a dislocation having both edge and screw components would be expected to induce a polarization structure with both vertical and horizontal components. This scenario suggests the possibility of realizing

*masuda.kairi.64n@st.kyoto-u.ac.jp
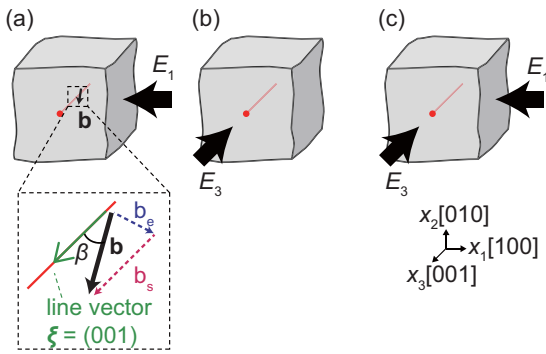
FIG. 1. Schematic illustrations of an ideal straight mixed dislocation (the red line) under (a) a uniaxial electric field $E_1$, (b) a uniaxial electric field $E_3$, and (c) a biaxial electric field $E_1 = E_3$. Here, $\mathbf{b}$, $b_e$, and $b_s$ are the Burgers vectors of the mixed dislocation, edge, and screw components, respectively, and $\beta$ is the angle between $\mathbf{b}$ and the line vector $\xi$. In this study, each dislocation was located on the [010] slip plane and $\xi$ was set to (001).

ferroelectricity that can be switched in multiple directions, which may allow logic calculations to be performed at the ultrasmall scale that the size reduction of external shapes cannot achieve.

Here, we assess the appearance of ferroelectricity around mixed dislocations in SrTiO$_3$ and demonstrate the possibility that these dislocations can function as ferroelectric nanoscale logic gates embedded in a paraelectric matrix. Phase-field simulations show that rectilinear polarization by the edge component and spiral polarization by the screw component of a mixed dislocation can be coupled due to the superposition of strain fields, resulting in a distorted spiral. Furthermore, the chirality of this spiral can be switched by applying an electric field that is both vertical and horizontal to the dislocation line. Based on this multidirectional switching, we demonstrate that OR, AND, and NOT operations can be performed by taking advantage of mixed dislocations in SrTiO$_3$. Our results provide a different strategy for the fabrication of ultrathin logic gates that may eventually lead to ultrahigh logic densities in conjunction with low-energy consumption.

## II. METHODS

Figure 1 shows schematic images of the dislocations employed in our simulation. In this study, the occurrence of ferroelectricity around mixed dislocations was examined by employing an ideal straight mixed dislocation. That is, the line vector $\xi$ was set to (001) and the Burgers vector, $\mathbf{b} =$ (001), was rotated on the slip plane [010], with $\beta$ being the angle between $\mathbf{b}$ and $\xi$. In the continuum mechanics, the Burgers vector of a mixed dislocation can be divided into an edge component, $b_e = |\mathbf{b}| \sin(\beta)$, and a screw component, $b_s = |\mathbf{b}| \cos(\beta)$ [29]. This mixed dislocation induces a strain concentration corresponding to the superposition of the strain fields associated with the edge (Fig. S1(b) in Supplemental Material Ref. [30]) and screw components (Fig. S1(b) in Supplemental Material Ref. [30]). This indicates that variations in $\beta$ affect the strain distribution which, in turn, modifies the ferroelectricity. Therefore, we employed mixed dislocations

with $\beta = 90°$ (that is, pure edge dislocations) to $0°$ (pure screw dislocations). To these ideal mixed dislocations, (i) a unidirectional electric field $E_1$ or (ii) $E_3$, or (iii) a biaxial electric field, $E_1 = E_3$, was applied [Figs. 1(a)–1(c)].

The reason why we employed ideal mixed dislocations is to make this study simple: Ordinarily, a mixed dislocation has a curved structure (Fig. S1(a) in Supplemental Material Ref. [30]) whose $\mathbf{b}$ is fixed due to the conservation law of the Burgers vector while the dislocation axis, that is, $\xi$, continuously rotates. Moreover, dislocations are not parallel to crystal orientations $x_1$[100], $x_2$[010], and $x_3$[001] due to the curved structure. Since polarization in SrTiO$_3$ favors pointing crystal orientations, this dislocation orientation variation affects ferroelectricity besides the elastic field transition between pure edge and screw dislocations. On the other hand, since SrTiO$_3$ is almost elastically isotropic, elastic fields around dislocations in the above ideal $\mathbf{b}$ rotated condition are the same as those in the actual $\xi$ rotated conditions. Moreover, in an ideal mixed dislocation, its axis is fixed and always parallel to the crystal orientation. Therefore, by employing an ideal mixed dislocation, we can eliminate dislocation orientation effects on ferroelectricity. Note that this ideal case may not be unrealistic because Furushima *et al.* recently demonstrated that straight mixed dislocations can be artificially generated in SrTiO$_3$ using a low-angle tilt grain boundary with a slight twist [31]. Furthermore, even if the effects of dislocation orientations are included, the following conclusion of this paper is not likely to change. This is because the Burgers vector of our main concern, i.e., pure edge and screw dislocations, and a mixed dislocation $\beta = 15°$ are parallel/almost parallel to the crystal orientations.

The formation of spontaneous polarization, $\boldsymbol{p} = (p_1, p_2, p_3)$, around the dislocation and the response of the polarization to the electric fields at room temperature were carefully simulated by phase-field modeling of SrTiO$_3$ based on the Ginzburg-Landau theory [32–37]. By this methodology, the $\mathbf{b}$ rotated condition can be easily realized. We employed a simulation model consisting of $128\Delta x \times 128\Delta x \times 4\Delta x$ grids ($\Delta x = 0.25$ nm) in which the elastic fields resulting from the mixed dislocations were introduced at the center (Fig. S2 in Supplemental Material Ref. [30]). Although a periodic boundary condition was applied to the model, the dislocations were considered to be isolated since the distance between neighboring dislocations was 32 nm. The phase-field simulations were performed using the Fourier spectral iterative perturbation method [38–41] and the semi-implicit Fourier spectral method [42,43] due to the computational efficiency of these techniques. Full details of the computations are provided in Supplemental Material 1 [30].

## III. RESULTS AND DISCUSSIONS

### A. Polarization distributions around dislocations

Figure 2 shows the polarization distributions around the mixed dislocations. Here, the contour regions indicate the locations at which ferroelectricity appeared. At $\beta = 90°$, that is, at the edge dislocation [Fig. 2(a)], a ferroelectric nanoscale region is evident immediately below the dislocation, having a size of approximately 6 nm. In this region, the
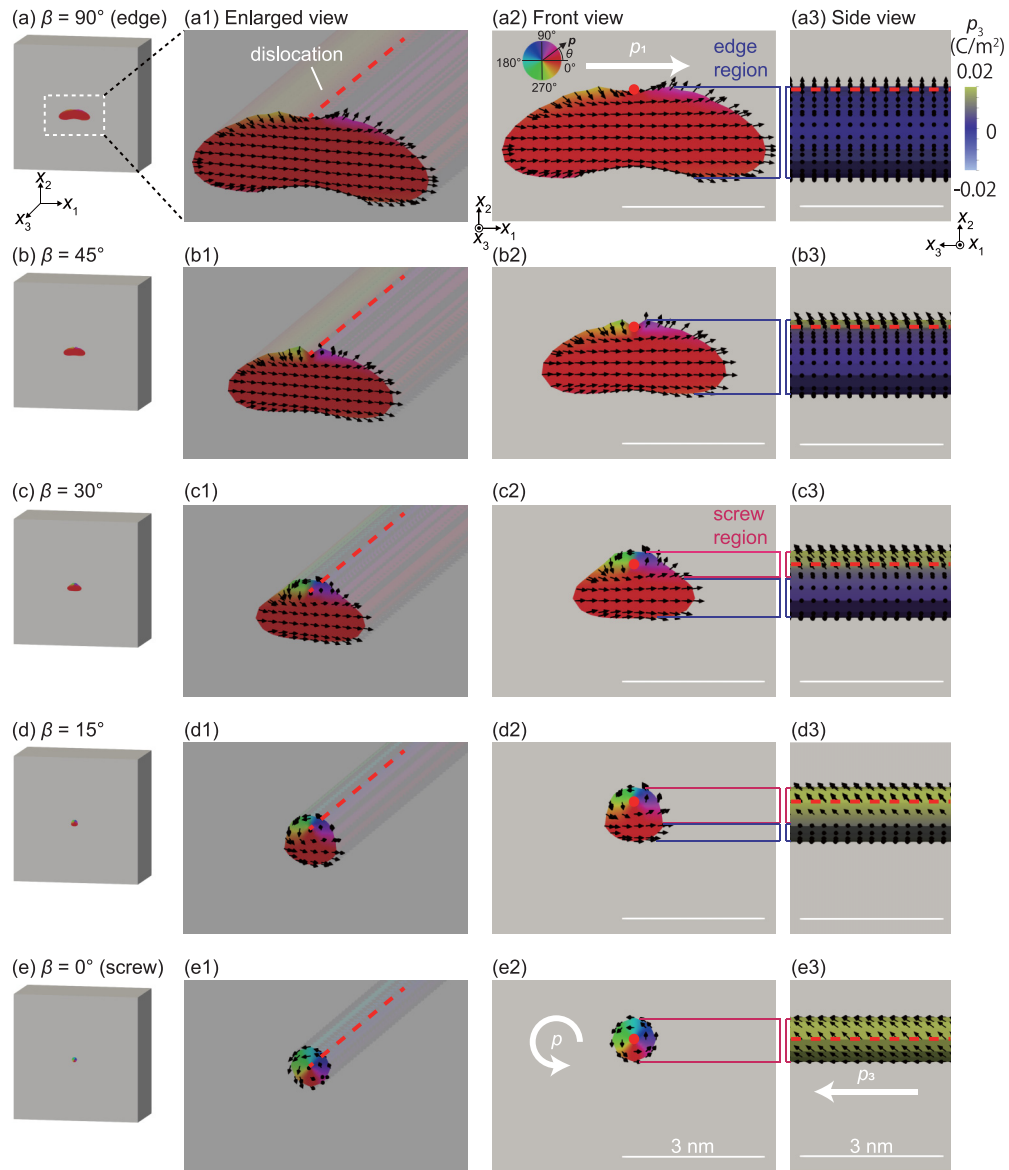
FIG. 2. Polarization distributions around mixed dislocations. In each figure, the contour region corresponds to $|\boldsymbol{p}| > 0.03$ C/m$^2$, and each scale bar indicates 3 nm. The colors indicate either the angle of polarization $\boldsymbol{p}$ or the magnitude of $p_3$, while the arrows denote the polarization directions. The edge region is that within which the polarization is primarily in the $x_1$ direction while the screw region is that within which the spiral polarization is dominant.

rectilinear polarization points in the $x_1$ direction [Fig. 2(a2)] and this polarization is induced by tensile strain around the edge dislocation [28]. In contrast, spiral polarization, that is, the coexistence of rectilinear polarization $p_3$ and polarization vortices, is induced around the screw dislocation $\beta = 0°$ as shown in Fig. 2(e), which can be attributed to the shear strain of this dislocation [28]. How shear strain induces ferroelectricity is further discussed in Supplemental Material 2 [30]. These configurations correspond to the polarization distributions obtained from *ab initio* calculations, that is, more exact calculations [28]. Therefore, regarding the strain-induced portion, the phase-field simulation successfully reproduces the appearance of ferroelectricity around the dislocations in SrTiO$_3$. Here, experiments have shown that polarization points radial directions around the edge dislocations at a low-angle grain boundary in SrTiO$_3$ [26]. This

discrepancy can be attributed to the superposition of strain. That is, since dislocations are very close to each other in a grain boundary, tensile and compressive regions around dislocations cancel each other. As a result, strain-induced ferroelectricity is reduced and other origins of ferroelectricity such as a Ti antisite become comparable. Note that, in the following text, the region incorporating $x_1$-directional rectilinear polarization is referred to as the edge region while that with spiral polarization is designated as the screw region.

The edge region formed at $\beta = 90°$ is seen to be reduced in size as $\beta$ is decreased, such that the size of the ferroelectric nanoscale region is decreased to approximately 4 nm at $\beta = 45°$ [Fig. 2(b2)]. In contrast, at $\beta = 30°$, a screw region is formed around the dislocation while the edge region further shrinks [Fig. 2(c2)]. As a result, a ferroelectric nanoscale region with both edge and screw parts is formed. At $\beta =$
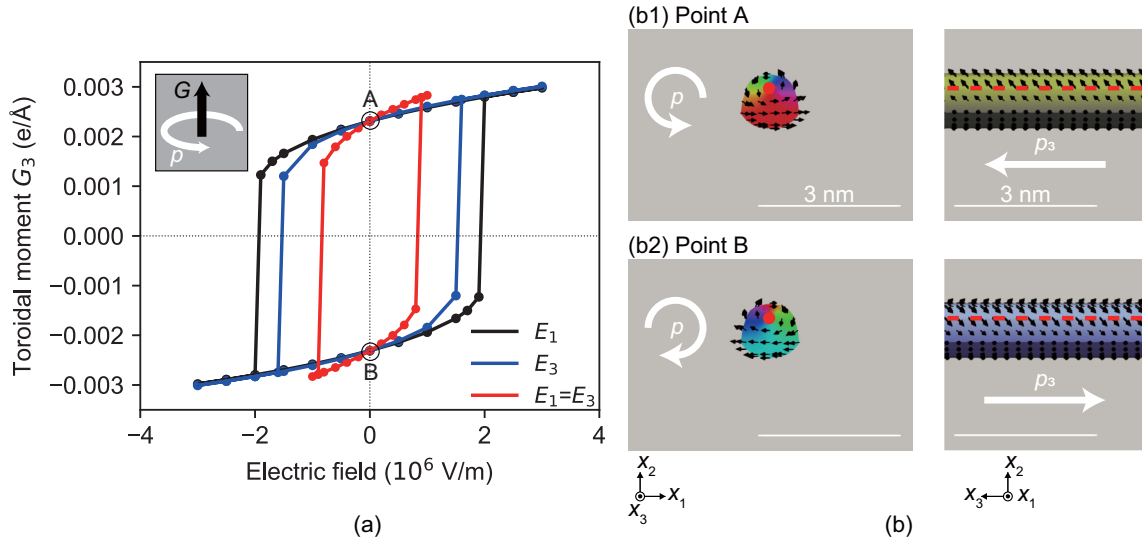
FIG. 3. (a) Hysteresis loops obtained from the mixed dislocation ($\beta = 15°$) under the uniaxial electric fields $E_x$, $E_z$ and biaxial electric field $E_x = E_z$. The diagram indicates a schematic illustration of the toroidal moment. (b) Polarization distributions at the corresponding points with scale bars being 3 nm.

15°, the edge region is further reduced in size, although the edge and screw regions still coexist [Fig. 2(d2)]. Finally, the ferroelectric nanoscale region comprises solely the screw region at $\beta = 0°$. This transition is attributed to the decrease in the tensile strain associated with the edge component with decreases in $\beta$, along with the concurrent increase in the shear strain associated with the screw component.

### B. Switching properties around mixed dislocations

Figure 3 shows the hysteresis loops obtained from a mixed dislocation with $\beta = 15°$. It should be noted that, due to a lack of experimental results, the core structures of mixed dislocations have not been fully clarified. However, a prior high-resolution transmission electron microscopy study of a twist boundary in $SrTiO_3$ established that a pure screw dislocation at a twist boundary does not show any remarkable variation from the ideal core structure [44]. Therefore, a mixed dislocation near a screw dislocation is likely not to deviate from the continuum mechanics and so we employed a mixed dislocation with $\beta = 15°$. Here, we assessed the response of the $x_3$ component of the toroidal moment $G$ described as [45,46]

$$G = \frac{1}{2V} \int_V r \times p \, dv, \qquad (1)$$

TABLE I. The coercive field values ($10^6$ V/m) for the average polarizations $P_1^{ave}$ and $P_3^{ave}$ (Supplemental Material 3 [30]) or toroidal moment $G_3$ around the edge, screw, and mixed dislocations. The $\times$ symbol indicates that the polarization or toroidal moment does not switch.

| Dislocation type | $E_1$ | $E_3$ | $E_1 = E_3$ |
|---|---|---|---|
| Edge ($\beta = 90°$) | 6.5 | $\times$ | 6.5 |
| Screw ($\beta = 0°$) | $\times$ | 0.5 | 0.4 |
| Mixed ($\beta = 15°$) | 1.9 | 1.5 | 0.8 |

where $r$ is the distance from the dislocation core and $V$ is the volume of the ferroelectric region. The same as a screw dislocation (Fig. S5 in Supplemental Material Ref. [30]), the chirality of the spiral can be switched by applying $E_3$ [the blue line in Figs. 3(a), 3(b1), and 3(b2)] and a hysteresis loop of the toroidal moment is obtained with a coercive field [47] of $1.5 \times 10^6$ V/m. Chirality switching in response to this homogeneous electric field is attributed to coupling of the in-plane and out-of-plane polarizations by the shear strain of the screw component (Supplemental Material 4 [30]). However, in contrast to a screw dislocation, the chirality can also be switched by applying $E_1$ with a coercive field of $1.9 \times 10^6$ V/m, as shown by the black line in Fig. 3(a). This is possible because switching in the edge region (Fig. S4 in Supplemental Material Ref. [30]) results in switching of the chirality. Therefore, the toroidal moment around the mixed dislocation can be switched by applying both $E_1$ and $E_3$. Furthermore, under a biaxial electric field, $E_1 = E_3$, the chirality is also switched even though a coercive field was $0.8 \times 10^6$ V/m, equal to approximately half the uniaxial electric field [the red

TABLE II. Truth tables obtained for a mixed dislocation ($\beta = 15°$). Values of 1 and 0 in the input column denote applying/not applying electric fields $E_1$ and $E_3$, while 1 and 0 in the output column denote whether the toroidal moment $G_3$ switches or does not switch.

| High electric field ($E_1, E_3 > 1.9 \times 10^6$ V/m) | | | Low electric field ($E_1, E_3 \approx 0.8 \times 10^6$ V/m) | | |
|---|---|---|---|---|---|
| Input | | Output | Input | | Output |
| $E_1$ | $E_3$ | $G_3$ | $E_1$ | $E_3$ | $G_3$ |
| 1 | 1 | 1 | 1 | 1 | 1 |
| 1 | 0 | 1 | 1 | 0 | 0 |
| 0 | 1 | 1 | 0 | 1 | 0 |
| 0 | 0 | 0 | 0 | 0 | 0 |
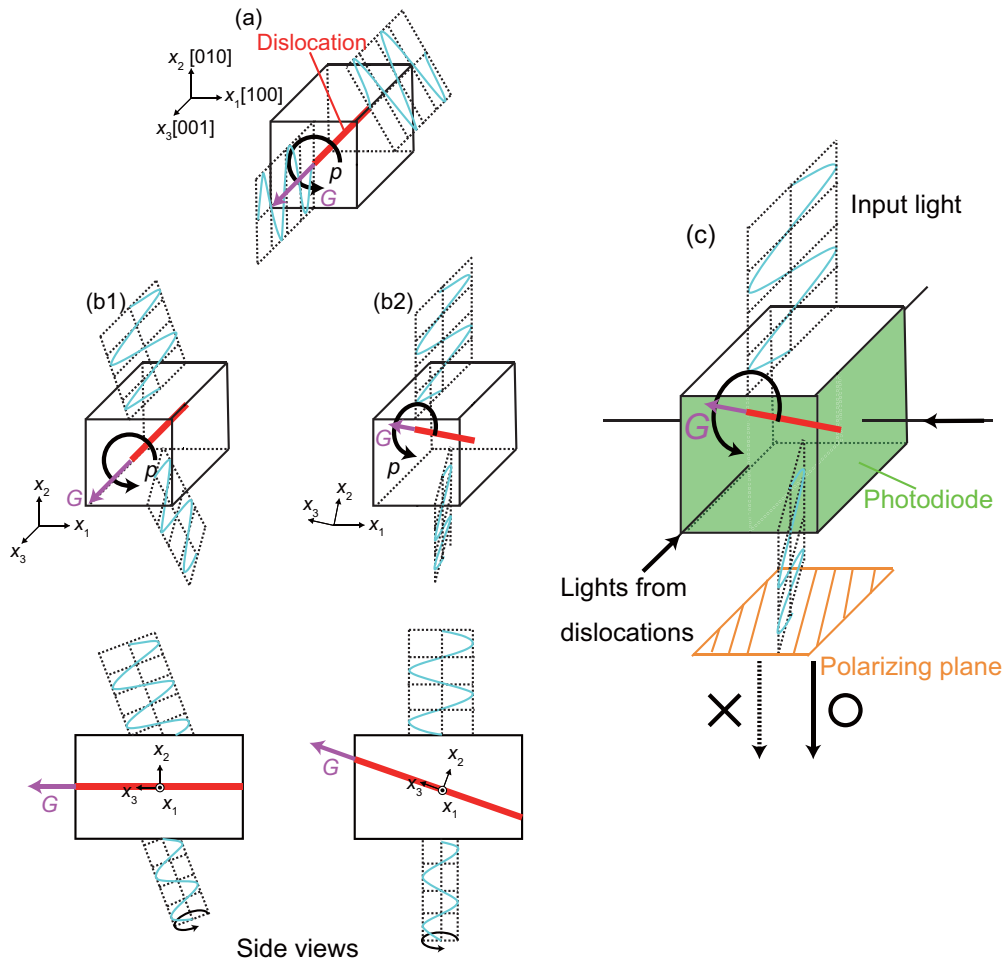
FIG. 4. Schematic illustrations of the rotation of light from (a) the front and (b) the side by polarization vortices around a mixed dislocation. (b1) Light or (b2) a dislocation is tilted. (c) A schematic illustration of a circuit utilizing the toroidal moments of a mixed dislocation.

line in Fig. 3(a)]. Therefore, the coercive field is significantly reduced when both $E_1$ and $E_3$ are applied at the same time. This phenomenon is not observed with the pure edge and screw dislocations. The coercive fields are summarized in Table I.

Note that, since the discovery of polarization vortices due to intensive surface effects in ferroelectric nanostructures [45], how to manipulate their vorticity has been a central issue [48–50]. Here, our study demonstrates that polarization vortices can be switched by two-directional homogeneous electric fields, which has never been reported to the best of our knowledge. On the other hand, this unusual switching property is apparently derived from strain fields specific to dislocations. This implies that as bulk and nanoscale ferroelectrics are different due to surface effects, nanoscale and ultrasmall ferroics are different due to unique properties of the defects. This will surely provide a different perspective on ferroics.

## C. Logic calculations by mixed dislocations

We subsequently investigated the feasibility of performing logic calculations based on a mixed dislocation with $\beta = 15°$. In this process, applying/not applying electric fields $E_1$ and $E_3$ are considered as an input of 1 and 0 while switching/not switching of the toroidal moment $G_3$ correspond to outputs of 1 and 0. As an example, in the case that $G_3$ is switched only under $E_1$, we will obtain $(E_1, E_3, G_3) = (1, 0, 1)$. Here, when the magnitude of the electric fields exceeds $1.9 \times 10^6$ V/m, $G_3$ is switched by both uniaxial and biaxial electric fields. However, when the magnitude of the electric fields is approximately $0.8 \times 10^6$ V/m, switching is induced only by the application of the biaxial electric fields, $E_1 = E_3$. These results are summarized in the truth tables provided in Table II. Under a high electric field ($>1.9 \times 10^6$ V/m), the output of an OR operation is obtained, while a low electric field (approximately $0.8 \times 10^6$ V/m) is equivalent to an AND operation. Therefore, the most basic logic calculations can be performed based on the appearance of ferroelectricity around a mixed dislocation. Additional observations of the ferroelectricity associated with a biaxial electric field, $-E_1 = E_3$, show no switching of the toroidal moment, indicating the possibility of a NOT operation (Supplemental Material 5 [30]). Therefore, this technique employing a mixed dislocation can provide a complete set of logic processes.

Since the ferroelectric nanoscale region is surrounded by paraelectric $SrTiO_3$, each mixed dislocation can be considered as a ferroelectric nanostructure embedded in a paraelectric

matrix, that is, as an isolated ferroelectric nanoscale logic gate within the host material. This represents a different route to fabricate ultrathin logic elements in nanodevices. As noted by Manipatruni *et al.*, utilizing ferroelectricity for logic gates may lead to energy-efficient devices due to the low-energy inputs required for polarization switching as well as the inherent nonvolatility [15]. In addition, a sufficiently high density of dislocations (up to $10^{12}$ cm$^{-2}$) has been introduced experimentally [51], indicating that a logic device with an ultrahigh density but low-power consumption can be realized. Note that the core idea of this study, that is, switching of polarization vortices at the screw region by homogeneous electric fields can be investigated by piezoresponse force microscopy. Moreover, the result of this study will surely stimulate further investigations of mixed dislocations in perovskite structures, which are much fewer than pure edge and screw dislocations.

### D. Proposal of a mixed dislocation circuit

Figure 4 shows schematic images of our proposal for a circuit that connects these dislocations. According to Prosandeev *et al.* [52], light through polarization vortices rotates. Therefore, light through a mixed dislocation with polarization vortices should rotate [Fig. 4(a)]. Note that this light rotation can be explained as the time variation of toroidal orders $d\mathbf{G}/dt$ by light induces magnetism and this magnetism, in turn, rotates light by Faraday effects. Therefore, this rotation should occur unless light and toroidal moments are perpendicular. In other words, light from the side also should rotate [Figs. 4(b1) and 4(b2)]. Based on this, we propose a nonvolatile logic circuitry as follows [Fig. 4(c)]: (1) We consider a dislocation with tilts while two sides are covered by photodiodes (conversion of light to electric voltage). (2) When light is supplied to this dislocation externally, this light should rotate due to the coupling with toroidal moments. (3) This light is judged by a polarizing plate. For example, light rotated clockwise can pass through the plate but light rotated anticlockwise cannot pass. (4) When this light passes, it reaches the next dislocation. This light can be converted to an electric voltage by photodiodes. Then this voltage switches polarization/does

not switch. (5) Whether polarization switches or not can be judged by supplying external light the same as in step (2) above. When polarization is switched, light passes through the polarizing plate and goes to the next dislocation. Note that this concept for constructing ultrasmall circuits is currently impractical or unlikely due to at least three reasons: First, to be comparable to the size of dislocations, i.e., <1 nm, a light source of x rays is needed. Second, whether x rays actually rotate by polarization vortices around a dislocation is still unclear. Third, preparing an x-ray-range photodiode and polarizer, and coating a dislocation with them are formidable tasks. Thus, at first, it is better to use low-angle grain boundaries in which dislocations array periodically (>100 nm) to avoid the problems related to x rays. Then, the next step is to gradually reduce the size to the single dislocation scale.

## IV. CONCLUSION

In summary, we have demonstrated the possibility that ferroelectric nanoscale logic gates can be achieved based on mixed dislocations in paraelectric SrTiO$_3$. Phase-field simulations showed that the strain concentration around a mixed dislocation induces a distorted spiral polarization whose chirality can be switched by applying both vertical and horizontal electric fields. Moreover, the coercive field required for switching is reduced by applying horizontal and vertical electric fields simultaneously. Using these switching properties, OR, AND, and NOT operations can be performed. Since the ferroelectric nanoscale region is a ferroelectric nanostructure embedded in a paraelectric matrix, a mixed dislocation represents a ferroelectric nanoscale logic gate within paraelectric SrTiO$_3$. This indicates a different approach to producing nanoscale logic elements with the potential to provide unprecedented densities and efficiency.

[1] K. J. Kuhn, Considerations for ultimate CMOS scaling, IEEE Trans. Electron Devices **59**, 1813 (2012).

[2] E. Pop, S. Sinha, and K. E. Goodson, Heat generation and transport in nanometer-scale transistors, Proc. IEEE **94**, 1587 (2006).

[3] V. V. Zhirnov and R. K. Cavin, Negative capacitance to the rescue?, Nat. Nanotechnol. **3**, 77 (2008).

[4] J. D. Meindl, Q. Chen, and J. A. Davis, Limits on silicon nanoelectronics for terascale integration, Science **293**, 2044 (2001).

[5] A. Danowitz, K. Kelley, J. Mao, J. P. Stevenson, and M. Horowitz, CPU DB: Recording microprocessor history, Commun. ACM **55**, 55 (2012).

[6] I. Ferain, C. A. Colinge, and J. P. Colinge, Multigate transistors as the future of classical metal-oxide-semiconductor field-effect transistors, Nature (London) **479**, 310 (2011).

[7] A. V. Chumak, A. A. Serga, and B. Hillebrands, Magnon transistor for all-magnon data processing, Nat. Commun. **5**, 4700 (2014).

[8] N. Kanazawa, T. Goto, K. Sekiguchi, A. B. Granovsky, C. A. Ross, H. Takagi, Y. Nakamura, H. Uchida, and M. Inoue, The role of Snell's law for a magnonic majority gate, Sci. Rep. **7**, 7898 (2017).

[9] B. Behin-Aein, D. Datta, S. Salahuddin, and S. Datta, Proposal for an all-spin logic device with built-in memory, Nat. Nanotechnol. **5**, 266 (2010).

[10] O. Zografos, S. Dutta, M. Manfrini, A. Vaysset, B. Sorée, A. Naeemi, P. Raghavan, R. Lauwereins, and I. P. Radu, Nonvolatile spin wave majority gate at the nanoscale, AIP Adv. **7**, 056020 (2017).

[11] S. Manipatruni, D. E. Nikonov, C. C. Lin, T. A. Gosavi, H. Liu, B. Prasad, Y. L. Huang, E. Bonturim, R. Ramesh, and I. A. Young, Scalable energy-efficient

magnetoelectric spin-orbit logic, Nature (London) **565**, 35 (2019).

[12] A. Imre, G. Csaba, L. Ji, A. Orlov, G. H. Bernstein, and W. Porod, Majority logic gate for magnetic quantum-dot cellular automata, Science **311**, 205 (2006).

[13] Z. Luo, A. Hrabec, T. P. Dao, G. Sala, S. Finizio, J. Feng, S. Mayr, J. Raabe, P. Gambardella, and L. J. Heyderman, Current-driven magnetic domain-wall logic, Nature (London) **579**, 214 (2020).

[14] J. F. Scott, Applications of modern ferroelectrics, Science **315**, 954 (2007).

[15] S. Manipatruni, D. E. Nikonov, and I. A. Young, Beyond CMOS computing with spin and polarization, Nat. Phys. **14**, 338 (2018).

[16] C. T. Nelson, P. Gao, J. R. Jokisaari, C. Heikes, C. Adamo, A. Melville, S. H. Baek, C. M. Folkman, B. Winchester, Y. Gu, Y. Liu, K. Zhang, E. Wang, J. Li, L. Q. Chen, C. B. Eom, D. G. Schlom, and X. Pan, Domain dynamics during ferroelectric switching, Science **334**, 968 (2011).

[17] M. J. Polking, M. G. Han, A. Yourdkhani, V. Petkov, C. F. Kisielowski, V. V. Volkov, Y. Zhu, G. Caruntu, A. P. Alivisatos, and R. Ramesh, Ferroelectric order in individual nanometre-scale crystals, Nat. Mater. **11**, 700 (2012).

[18] D. D. Fong, G. B. Stephenson, S. K. Streiffer, J. A. Eastman, O. Auciello, P. H. Fuoss, and C. Thompson, Ferroelectricity in ultrathin perovskite films, Science **304**, 1650 (2004).

[19] J. Junquera and P. Ghosez, Critical thickness for ferroelectricity in perovskite ultrathin films, Nature (London) **422**, 506 (2003).

[20] S. Miyazawa, Y. Ishii, S. Ishida, and Y. Nanishi, Direct observation of dislocation effects on threshold voltage of a GaAs field-effect transistor, Appl. Phys. Lett. **43**, 853 (1983).

[21] S. P. Alpay, I. B. Misirlioglu, V. Nagarajan, and R. Ramesh, Can interface dislocations degrade ferroelectric properties? Appl. Phys. Lett. **85**, 2044 (2004).

[22] M. W. Chu, I. Szafraniak, R. Scholz, C. Harnagea, D. Hesse, M. Alexe, and U. Gösele, Impact of misfit dislocations on the polarization instability of epitaxial nanostructured ferroelectric perovskites, Nat. Mater. **3**, 87 (2004).

[23] J. H. Haeni, P. Irvin, W. Chang, R. Uecker, P. Reiche, Y. L. Li, S. Choudhury, W. Tian, M. E. Hawley, B. Craigo, A. K. Tagantsev, X. Q. Pan, S. K. Streiffer, L. Q. Chen, S. W. Kirchoefer, J. Levy, and D. G. Schlom, Room-temperature ferroelectricity in strained SrTiO₃, Nature (London) **430**, 758 (2004).

[24] H. Uwe and T. Sakudo, Stress-induced ferroelectricity and soft phonon modes in SrTiO₃, Phys. Rev. B **13**, 271 (1976).

[25] A. Vasudevarao, A. Kumar, L. Tian, J. H. Haeni, Y. L. Li, C. J. Eklund, Q. X. Jia, R. Uecker, P. Reiche, K. M. Rabe, L. Q. Chen, D. G. Schlom, and V. Gopalan, Multiferroic Domain Dynamics in Strained Strontium Titanate, Phys. Rev. Lett. **97**, 257602 (2006).

[26] P. Gao, S. Yang, R. Ishikawa, N. Li, B. Feng, A. Kumamoto, N. Shibata, P. Yu, and Y. Ikuhara, Atomic-Scale Measurement of Flexoelectric Polarization at SrTiO₃ Dislocations, Phys. Rev. Lett. **120**, 267601 (2018).

[27] K. Masuda, L. V. Lich, T. Shimada, and T. Kitamura, Periodically-arrayed ferroelectric nanostructures induced by dislocation structures in strontium titanate, Phys. Chem. Chem. Phys. **21**, 22756 (2019).

[28] T. Shimada, K. Masuda, Y. Hagiwara, N. Ozaki, T. Xu, J. Wang, and T. Kitamura, Ferroic dislocations in paraelectric SrTiO₃, Phys. Rev. B **103**, L060101 (2021).

[29] J. P. Hirth and J. Lothe, *Theory of Dislocations* (Krieger, Malabar, FL, 1982).

[30] See Supplemental Material at http://link.aps.org/supplemental/10.1103/PhysRevB.104.054104 for simulation details, ferroelectricity induced by shear strain, hysteresis loops around edge and screw dislocations, chirality switching mechanism around a screw dislocation, and toroidal moments $G_3$ under $-E_1 = E_3$.

[31] Y. Furushima, Y. Arakawa, A. Nakamura, E. Tochigi, and K. Matsunaga, Nonstoichiometric [012] dislocation in strontium titanate, Acta Mater. **135**, 103 (2017).

[32] G. Sheng, Y. L. Li, J. X. Zhang, S. Choudhury, Q. X. Jia, V. Gopalan, D. G. Schlom, Z. K. Liu, and L. Q. Chen, Phase transitions and domain stabilities in biaxially strained (001) SrTiO₃ epitaxial thin films, J. Appl. Phys. **108**, 084113 (2010).

[33] G. Sheng, Y. L. Li, J. X. Zhang, S. Choudhury, Q. X. Jia, V. Gopalan, D. G. Schlom, Z. K. Liu, and L. Q. Chen, A modified Landau-Devonshire thermodynamic potential for strontium titanate, Appl. Phys. Lett. **96**, 232902 (2010).

[34] Y. L. Li, S. Choudhury, J. H. Haeni, M. D. Biegalski, A. Vasudevarao, A. Sharan, H. Z. Ma, J. Levy, V. Gopalan, S. Trolier-McKinstry, D. G. Schlom, Q. X. Jia, and L. Q. Chen, Phase transitions and domain structures in strained pseudocubic (100) SrTiO₃ thin films, Phys. Rev. B **73**, 184112 (2006).

[35] G. Shirane and Y. Yamada, Lattice-dynamical study of the 110° K phase transition in SrTiO₃, Phys. Rev. **177**, 858 (1969).

[36] B. K. Choudhury, K. V. Rao, and R. N. P. Choudhury, Dielectric properties of SrTiO₃ single crystals subjected to high electric fields and later irradiated with X-rays or γ-rays, J. Mater. Sci. **24**, 3469 (1989).

[37] H. H. Wu, J. Wang, S. G. Cao, L. Q. Chen, and T. Y. Zhang, Micro-/macro-responses of a ferroelectric single crystal with domain pinning and depinning by dislocations, J. Appl. Phys. **114**, 164108 (2013).

[38] J. J. Wang, X. Q. Ma, Q. Li, J. Britson, and L. Q. Chen, Phase transitions and domain structures of ferroelectric nanoparticles: Phase field model incorporating strong elastic and dielectric inhomogeneity, Acta Mater. **61**, 7591 (2013).

[39] J. J. Wang, Y. Song, X. Q. Ma, L. Q. Chen, and C. W. Nan, Static magnetic solution in magnetic composites with arbitrary susceptibility inhomogeneity and anisotropy, J. Appl. Phys. **117**, 043907 (2015).

[40] P. Yu, S. Y. Hu, L. Q. Chen, and Q. Du, An iterative-perturbation scheme for treating inhomogeneous elasticity in phase-field models, J. Comput. Phys. **208**, 34 (2005).

[41] P. Song, T. Yang, Y. Ji, Z. Wang, Z. Yang, L. Q. Chen, and L. Chen, A comparison of Fourier spectral iterative perturbation method and finite element method in solving phase-field equilibrium equations, Commun. Comput. Phys. **21**, 1325 (2017).

[42] L. Q. Chen and J. Shen, Applications of semi-implicit Fourier-spectral method to phase field equations, Comput. Phys. Commun. **108**, 147 (1998).

[43] H. L. Hu and L. Q. Chen, Three-dimensional computer simulation of ferroelectric domain formation, J. Am. Ceram. Soc. **81**, 492 (1998).

[44] Z. Zhang, W. Sigle, and W. Kurtz, HRTEM and EELS study of screw dislocation cores in SrTiO$_3$, Phys. Rev. B **69**, 144103 (2004).

[45] I. I. Naumov, L. Bellaiche, and H. Fu, Unusual phase transitions in ferroelectric nanodisks and nanorods, Nature (London) **432**, 737 (2004).

[46] V. M. Dubovik and V. V. Tugushev, Toroid moments in electrodynamics and solid-state physics, Phys. Rep. **187**, 145 (1990).

[47] V. Janovec, On the theory of the coercive field of single-domain crystals of BaTiO$_3$, Czech. J. Phys. **8**, 3 (1958).

[48] S. Prosandeev, I. Ponomareva, I. Kornev, and L. Bellaiche, Control of Vortices by Homogeneous Fields in Asymmetric Ferroelectric and Ferromagnetic Rings, Phys. Rev. Lett. **100**, 047201 (2008).

[49] L. V. Lich, T. Shimada, J. Wang, V. H. Dinh, T. Q. Bui, and T. Kitamura, Switching the chirality of a ferroelectric vortex in designed nanostructures by a homogeneous electric field, Phys. Rev. B **96**, 134119 (2017).

[50] J. Wang, Switching mechanism of polarization vortex in single-crystal ferroelectric nanodots, Appl. Phys. Lett. **97**, 192901 (2010).

[51] I. Sugiyama, N. Shibata, Z. Wang, S. Kobayashi, T. Yamamoto, and Y. Ikuhara, Ferromagnetic dislocations in antiferromagnetic NiO, Nat. Nanotechnol. **8**, 266 (2013).

[52] S. Prosandeev, A. Malashevich, Z. Gui, L. Louis, R. Walter, I. Souza, and L. Bellaiche, Natural optical activity and its control by electric field in electrotoroidic systems, Phys. Rev. B **87**, 195111 (2013).